Structural Engineering and Mechanics, *Vol. 53, No. 4 (2015) 645-659*
DOI: http://dx.doi.org/10.12989/sem.2015.53.4.645

Thermoelastic analysis for a slab made of a thermal diode-like material

Feras H. Darwish*[1], Mohammad A. Al-Nimr[2] and Mohammad I. Hatamleh[2]

[1]*Aeronautical Engineering Department, Jordan University of Science and Technology, Irbid 22110, Jordan*
[2]*Mechanical Engineering Department, Jordan University of Science and Technology, Irbid 22110, Jordan*

(Received January 8, 2014, Revised July 8, 2014, Accepted July 13, 2014)

Abstract. This research investigates the thermoelastic transient behavior of a thermally loaded slab made of a thermal diode-like material which has two directional thermal conductivity values (low and high). Finite difference analysis is used to obtain the elastic response of the slab based on the temperature solutions. It is found that the rate of heat transfer through the thickness of the slab decreases with reducing the ratio between the low and high thermal conductivity values (R). In addition, reducing R makes the slab less responsive to the thermal load when heated from the direction associated with the low thermal conductivity value.

Keywords: thermal diode like material; thermoelastic transient response; finite difference analysis; low-to-high thermal conductivity ratio

1. Introduction

A thermal diode like material conceptually allows the heat flux in one direction and acts like an insulator when the temperature gradient is reversed. Practically a thermal diode material conducts the heat flux more efficiently in one direction than in the reversed direction, or in other words possesses a directional thermal conductivity values, high and low. The fabrication of such materials can virtually revolutionize many industrial, mechanical and climate control processes requiring extremely high levels of heat resistance and heat flux direction-control. For example, thermal diode materials can serve many applications such as in the construction and building management where heating, air conditioning and rapid hot water delivery are of great importance; in refrigeration systems, heat exchangers and as insulation materials.

In general the area of thermal stresses was investigated by many researchers. Boley and Weiner (1985) used the diffusion heat conduction model in their thermal stress analysis. Nowacki (1986) presented the different thermoelastic responses of plates that are subjected to various thermal loads. The subject of lagging behavior of heat transport in both rigid and deformable bodies was addressed by Tzou (1997). Al-Huniti *et al*. (2001) studied the dynamic thermal stresses and deformations in a thin rod due to a moving heat source using the hyperbolic heat conduction model. Al-Huniti and Al-Nimr (2000), Suh and Burger (1998) assumed the validity of the

*Corresponding author, Associate Professor, E-mail: fhdarwish@just.edu.jo

http://www.techno-press.org/?journal=sem&subpage=8 ISSN: 1225-4568 (Print), 1598-6217 (Online)

hyperbolic heat conduction model to investigate the thermal stresses within thin plates exposed to a fast heating rate. Al-Nimr and Al-Huniti (2000) investigated the transient thermal stresses generated within a thin homogeneous plate as a result of a fast rate of heating using dual-phase-lag heat conduction model. The thermal stresses along cylindrical rods subjected to an instantaneous heating was studied by Hata (2001). Addam (2000) studied the temperature and thermal stresses in a two-layer slab under the effect of the hyperbolic heat conduction model. Tall (1964) presented a method for the calculation of thermal and residual stresses produced in individual plates due to welding. Sumi *et al*. (1987) predicted the thermal stresses due to a moving local heat source of finite dimension over the surface of an infinite elastic slab. Al-Nimr and Abou-Arab (1994) studied the transient heat conduction process with a moving heat source simulating a welding process. Darwish *et al*. (2012) investigated the transient response of clamped thin slap under pressure and thermal loads through analytical and finite difference approaches. The area of modeling and studying the behavior of thermal diode like materials attracted few researchers. Li *et al*. (2004, 2006) presented a theoretical model for a thermal transistor based on the phenomenon of negative differential thermal resistance observed in thermal diode material. The thermal transistor is a three-terminal device with the important feature that the current through the two terminals can be controlled by small changes in the temperature or in the current through the third terminal. This control feature allows switching the device between “off” (insulating) and “on” (conducting) states or to amplify a small current. They also presented a model of a thermal diode by using two coupled nonlinear lattices. Terraneo *et al*. (2002) investigated the possibility to control the energy transport inside a nonlinear one-dimension chain connecting with two thermostats at different temperatures. They emphasized that controlling heat conduction by nonlinearity opens a new possibility to design a thermal rectifier, i.e., a lattice that carries heat preferentially in one direction. Hu *et al*. (2005) investigated the heat conduction in one dimensional chains. It is found that the heat fluxes along opposite directions can be significantly different. They also stated that one can control the heat flux through the external potential, which can induce a conductor-insulator transition of the system.

The main objective of this research is to study the transient thermoelastic behavior of a slab made of a thermal diode-like material when subjected to a thermal load. Ieşan (2008) presented the solution of the equilibrium problem for a right cylinder which is subject to a prescribed thermal field and resultant forces and resultant moments on the ends. Shahani and Bashusqeh (2013) solved analytically a coupled thermo-elasticity problem in a thick-walled sphere using an innovative technique in conjunction with the finite Hankel transform. Feng *et al*. (2008) studied the mechanical behavior induced by a penny-shaped crack in a magneto-electro-thermal-elastic layer that is subjected to a heat flow. Numerical solutions for the temperature, displacement and stress distributions were obtained by Brischetto *et al*. (2008) for a simply supported rectangular functionally graded plate subjected to thermo-mechanical bending load. Xu *et al*. (2010) proposed an approximate analytical solution method to study the three-dimensional thermoelastic behavior of rectangular plates with variable thickness when subjected to thermo-mechanical loads.

2. Description of the problem

A clamped-free infinite width slab of length (L) and thickness (h) is considered for the analysis of this research. The slab is made of a thermal diode-like material that has a directional thermal conductivity property, the value of which (low or high) is determined by the direction of the heat

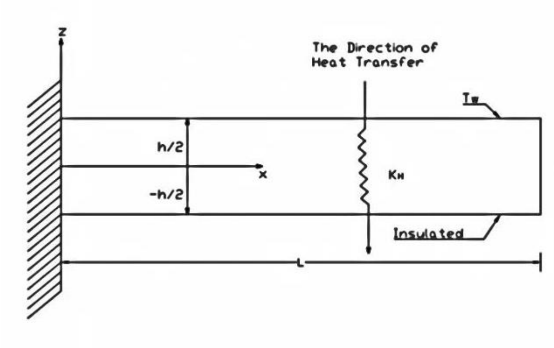

(a) Case (1): high thermal conductivity (k_H)

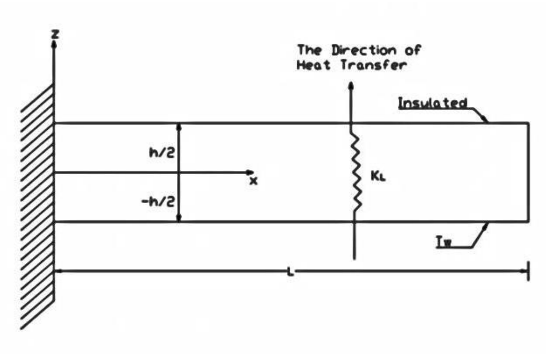

(b) Case (2): low thermal conductivity (k_L)

Fig. 1 Geometric and load configurations of the slab

flow. Figs. 1(a) and 1(b) show cases (1) and (2) of the analysis respectively. In case (1), the heat flow is directed from the isothermal upper side of the slab to the insulated lower side with the high value of the thermal conductivity of the material (k_H). In case (2), the heat flow direction and the thermal boundary conditions across the thickness of the slab are reversed and hence the thermal conductivity of the material is switched to the low value (k_L).

3. The governing equations

The equations that describe the current problem are divided into two parts: (1) the thermal equations, and (2) the thermoelastic equations. The following subsections present the details of each part.

3.1 The thermal equations

The transient 1-D heat conduction model along with the initial and boundary conditions of case (1) of the analysis are expressed in Eqs. (1)-(2) respectively, Kreith and Black (1980).

$$\frac{\partial T}{\partial t} = \alpha_H \frac{\partial^2 T}{\partial z^2} \tag{1}$$

$$\begin{bmatrix} T(z,0) = T_\infty \\ T\left(\frac{h}{2}, t\right) = T_w \\ \left(\left.\frac{dT}{dz}\right|_{z=\frac{-h}{2}}\right) = 0 \end{bmatrix} \tag{2}$$

For case (2), the temperature gradient is reversed, the thermal conductivity of the material turns to low and the thermal diode effect appears. The governing thermal equation and the corresponding initial and boundary conditions are presented in Eqs. (3)-(4)

$$\frac{\partial T}{\partial t} = \alpha_L \frac{\partial^2 T}{\partial z^2} \tag{3}$$

$$\begin{bmatrix} T(z,0) = T_\infty \\ T\left(\frac{-h}{2}, t\right) = T_w \\ \left(\left.\frac{dT}{dz}\right|_{z=\frac{h}{2}}\right) = 0 \end{bmatrix} \tag{4}$$

The ratio between the low and high thermal conductivity of the material is denoted by R and expressed as $R=k_L/k_H$. Accordingly, Eq. (3) can be written in the new form as in Eq. (5).

$$\frac{\partial T}{\partial t} = R\alpha_H \frac{\partial^2 T}{\partial z^2} \tag{5}$$

To express the above equations in a dimensionless parametric form, the following dimensionless parameters are defined

$$\left[\theta = \frac{T - T_\infty}{T_w - T_\infty} \ \ , \ \xi = \frac{z}{h} \ \ , \ \ \eta = \frac{t\,\alpha_H}{h^2}\ \right] \tag{6}$$

Subsequently, the dimensionless expressions of Eqs. (1), (2), (5) and (4) are written as in Eqs. (7), (8), (9) and (10) respectively.

$$\frac{\partial \theta}{\partial \eta} = \frac{\partial^2 \theta}{\partial \xi^2} \tag{7}$$

$$\begin{bmatrix} \theta(\xi,0) = 0 \\ \theta\left(\frac{1}{2}, \eta\right) = 1 \\ \frac{d\theta(-\frac{1}{2},\eta)}{d\xi} = 0 \end{bmatrix} \tag{8}$$

$$\frac{\partial \theta}{\partial \eta} = R\frac{\partial^2 \theta}{\partial \xi^2} \tag{9}$$

$$\begin{bmatrix} \theta(\xi,0) = 0 \\ \theta\left(-\frac{1}{2}, \eta\right) = 1 \\ \frac{d\theta(\frac{1}{2},\eta)}{d\xi} = 0 \end{bmatrix} \tag{10}$$

3.2 The thermoelastic equations

The problem under investigation is described as a thermo-mechanically coupled problem as the heat conduction solution driven by the boundary conditions directly affects the mechanical behavior of the solid component. Specifically, the thermoelastic response of the slab is primarily based on the incorporation of the applied thermal load resulting from the temperature distribution through the thickness of the slab into the equilibrium equation or into the equation of motion, if the transient response is needed, in order to obtain the deflection caused by the thermal load. Subsequently, the compatibility and the constitutive equations of solid mechanics can be implemented to obtain the thermal strain and stress distributions of the thermally loaded component. In the current problem, the transient response of the slab due to the thermal load in terms of the transverse deflection and the generated stresses and strains will be obtained by solving the equation of motion taking into consideration the geometric boundary and initial conditions. The partial differential equation of the transverse deflection of a clamped-free slab subjected to a thermal load and the corresponding boundary and initial conditions are expressed in Eqs. (11) and (12), Ugural (1999).

$$D\frac{\partial^4 w}{\partial x^4}+\rho h\frac{\partial^2 w}{\partial t^2}=-\frac{1}{1-\upsilon}\frac{\partial^2 M_T}{\partial x^2} \tag{11}$$

$$\begin{bmatrix} w(x,0)=0 \\ \dfrac{\partial w(x,0)}{\partial t}=0 \\ w(0,t)=0 \\ \dfrac{\partial w(0,t)}{\partial x}=0 \\ \dfrac{\partial^2 w(L,t)}{\partial x^2}=-\dfrac{M_T}{(1-\upsilon)D} \\ \dfrac{\partial^3 w(L,t)}{\partial x^3}=0 \\ \dfrac{\partial^4 w(L,t)}{\partial x^4}=0 \end{bmatrix} \tag{12}$$

The right hand side of Eq. (11) represents the thermal load, where (M_T) is the thermal moment and can be obtained by performing the integration of Eq. (13)

$$\mathrm{M_{T}}=\gamma\mathrm{E}\int_{-\mathrm{h}/2}^{\mathrm{h}/2}[\mathrm{T(z,t)}-\mathrm{T_\infty}]\mathrm{zdz} \tag{13}$$

Due to the thermal load, stress and strain domains will be generated and can be obtained at any time and thickness location by using the following equations

$$\sigma_T=\frac{-E(1+\upsilon)\gamma(T(z,t)-T_\infty)}{(1-\upsilon^2)} \tag{14}$$

$$\varepsilon_T=\gamma(T(z,t)-T_\infty) \tag{15}$$

The above thermoelastic equations can be represented in dimensionless form by applying the following non-dimensional parameters

$$\begin{bmatrix} W=\dfrac{w}{L}\ , \quad X=\dfrac{x}{L}\ , \quad \mu=\dfrac{\alpha^2\rho L^4}{Dh^3}, \\ AR=\dfrac{L}{h}\ , \quad \lambda=12\gamma(1+\upsilon)(T_w-T_\infty)AR \\ S_T=\dfrac{(1-\upsilon)\sigma_T}{\gamma E(T_w-T_\infty)}\ , \quad \epsilon_T=\dfrac{\varepsilon_T}{\gamma(T_w-T_\infty)} \end{bmatrix} \tag{16}$$

The resulting dimensionless governing equation, initial and boundary conditions, thermal moment, thermal stress and thermal strain are expressed in Eqs. (17)-(21) respectively

$$\left[\frac{\partial^4 W}{\partial X^4} + \mu \frac{\partial^2 W}{\partial \eta^2} = -\frac{L}{(1-v)D}\frac{\partial^2 M_T}{\partial X^2}\right] \tag{17}$$

$$\left[\begin{array}{c} W(X,0) = 0 \\ \frac{\partial W(X,0)}{\partial \eta} = 0 \\ W(0,\eta) = 0 \\ \frac{\partial W(0,\eta)}{\partial X} = 0 \\ \frac{\partial^2 W(1,\eta)}{\partial X^2} = -\lambda \int_{-1/2}^{1/2} \theta(\xi,\eta)\xi.\,d\xi \\ \frac{\partial^3 W(1,\eta)}{\partial X^3} = 0 \\ \frac{\partial^4 W(1,\eta)}{\partial X^4} = 0 \end{array}\right] \tag{18}$$

$$M_{T=}\gamma E(T_w - T_\infty) \int_{-1/2}^{1/2} \theta(\xi,\eta)\xi.\,d\xi \tag{19}$$

$$S_T(\xi,\eta) = -\theta(\xi,\eta) \tag{20}$$

$$\epsilon_T(\xi,\eta) = \theta(\xi,\eta) \tag{21}$$

4. Temperature and deflection solutions

The transient solution of the temperature through the thickness of the slab is obtained for cases (1) and (2) by analytically solving Eqs. (7) and (9) respectively. The method of separation of variables along with Fourier series representation is used to obtain the solutions as presented in Eqs. (22)-(23) for cases (1) and (2) respectively.

$$\theta(\xi,\eta) = 1 - \sum_{m=1}^{\infty} \frac{2}{\beta_m} \sin\left(\frac{\beta_m}{2}\right) * e^{-\beta_m{}^2\eta}\,[cos(\beta_m\xi) + (-1)^m sin(\beta_m\xi)] \tag{22}$$

$$\theta(\xi,\eta) = 1 - \sum_{m=1}^{\infty} \frac{2}{\beta_m} \sin\left(\frac{\beta_m}{2}\right) * e^{-R\beta_m{}^2\eta}\,[cos(\beta_m\xi) + (-1)^{m+1} sin(\beta_m\xi)] \tag{23}$$

The above solutions are part of the thermoelastic analysis as the dimensionless temperature appears in the thermal moment term and one of the boundary conditions.

It is obvious now that thermal moment is independent of the longitudinal distance X, accordingly, the right hand side of Eq. (17) turns to zero and the new equation of motion is written below

$$\frac{\partial^4 W}{\partial X^4} + \mu \frac{\partial^2 W}{\partial \eta^2} = 0 \tag{24}$$

The above equation along with the associated initial and boundary conditions of Eq. (18) is solved numerically by implementing the finite difference techniques for discretization, mesh refinement, and solution convergence and by using FORTRAN commercial software in order to obtain the transient-to-steady state solutions of the deflection, $W(X, \eta)$. In addition, the steady state solution is obtained analytically by solving the equilibrium equation which is derived from Eq. (24) by substituting zero for the second derivative with respect to time $\left(\frac{\partial^2 W}{\partial \eta^2} = 0\right)$. The dimensionless analytical solution of the transverse deflection is expressed in Eq. (25) and is used to verify the steady state finite difference solution.

$$W(X) = \frac{-\lambda * X^2}{2} \int_{-1/2}^{1/2} \theta(\xi, \eta)\xi . d\xi \tag{25}$$

5. Results and discussion

This section presents the analytical and the finite difference results which primarily focus on the temperature distributions through the thickness of the slab and the effect of the thermal diode like property of the material on the thermoelastic response of the slab in terms of deflection, strain and stress.

The analytical solution of the transient dimensionless temperature through the thickness of the slab is shown in Figs. 2 and 3 for cases (1) and (2) respectively.

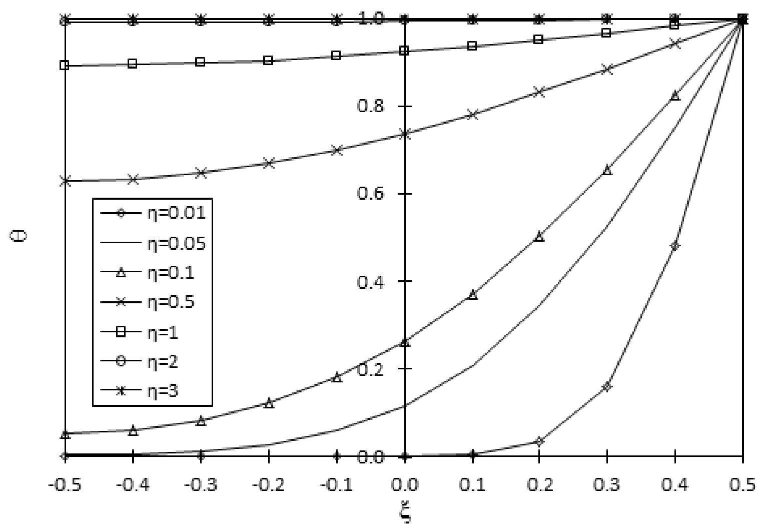

Fig. 2 Variation of the transient dimensionless temperature distribution through the thickness of the slab under thermal load for case (1)

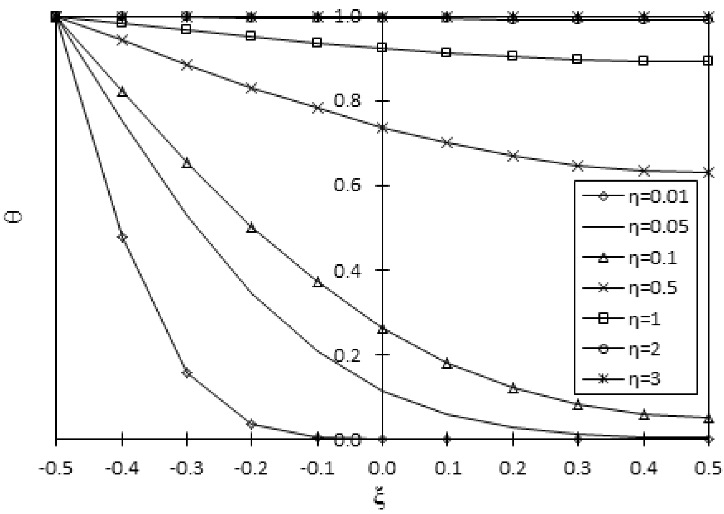

Fig. 3 Variation of the transient dimensionless temperature distribution through the thickness of the slab under thermal load for case (2) (R=1)

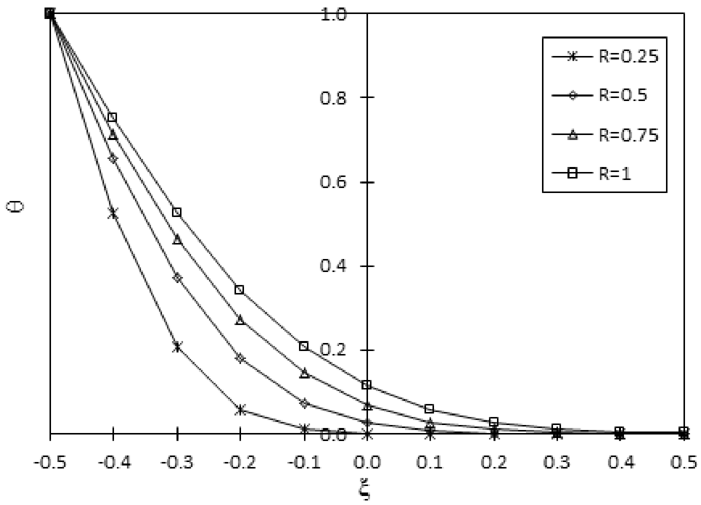

Fig. 4 The transient dimensionless temperature distributions through the thickness of the slab at η =0.05

As shown in Fig. 2, at any time of the transient solution, the dimensionless temperature remains constant at θ =1 at the upper surface (ξ=0.5) and the temperature gradient remains zero $\left(\frac{\partial\theta}{\partial\xi} = 0\right)$ at the lower surface (ξ=-0.5). These results are forced by the boundary conditions. It is also observed that the steady state time at which the temperature becomes uniform (θ =1) is η_{ss}=3. Fig. 3 is basically a reversed version of Fig. 2 since the boundary conditions and the heat flow are reversed while maintaining R=1. In addition, Figs. 2 and 3 show that the dimensionless time (η) at which the value of θ at the insulated side of the slab departs from 0 is around 0.05. This value changes with varying R as will be shown later and is defined hereinafter as the critical time (η_c).

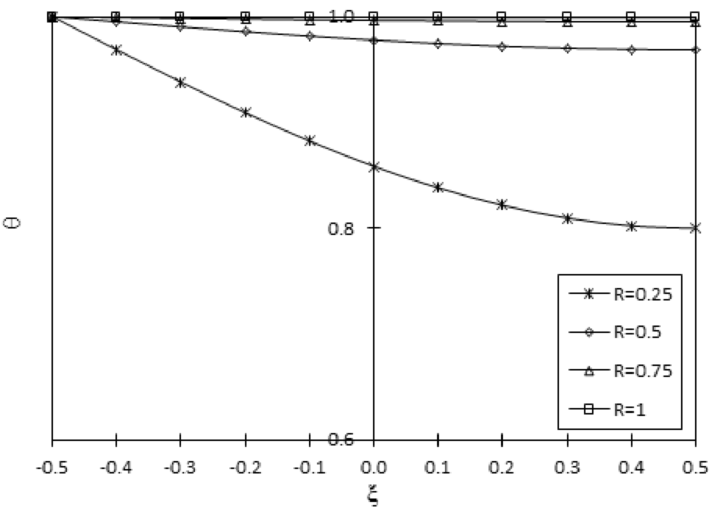

Fig. 5 The transient dimensionless temperature distributions through the thickness of the slab at η =3

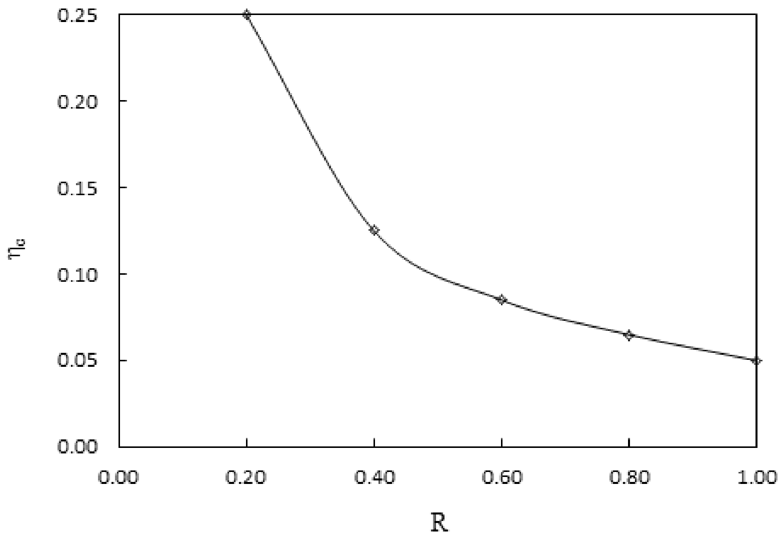

Fig. 6 The effect of thermal conductivity ratio (R) on the critical time (η_c)

Figs. 4 and 5 present the dimensionless temperature distributions for case (2) at different ratios of R when η=0.05 and 3 respectively.

It is observed in Figs. 4 and 5 that by decreasing the value of R the rate of heat transfer becomes slower and therefore the transient time becomes longer. This effect is clearly shown in Figs. 6 and 7 which present the direct effect of R on the critical time and steady state time of the dimensionless temperature distribution respectively.

From Figs. 6 and 7, it is obvious that by decreasing the value of R form 1 to 0.2, the rate of heat transfer becomes approximately 5 to 6 times slower.

The thermoelastic response of the clamped-free slab under consideration which is subjected to a

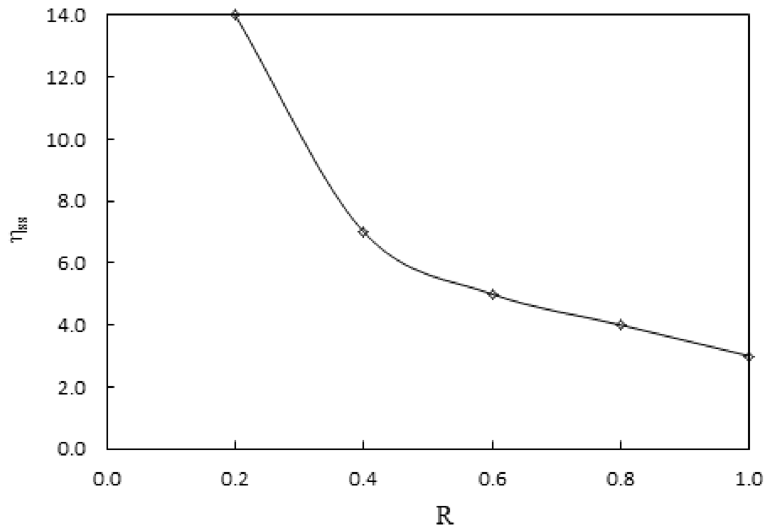

Fig. 7 The effect of thermal conductivity ratio (R) on the steady state time (η_{ss})

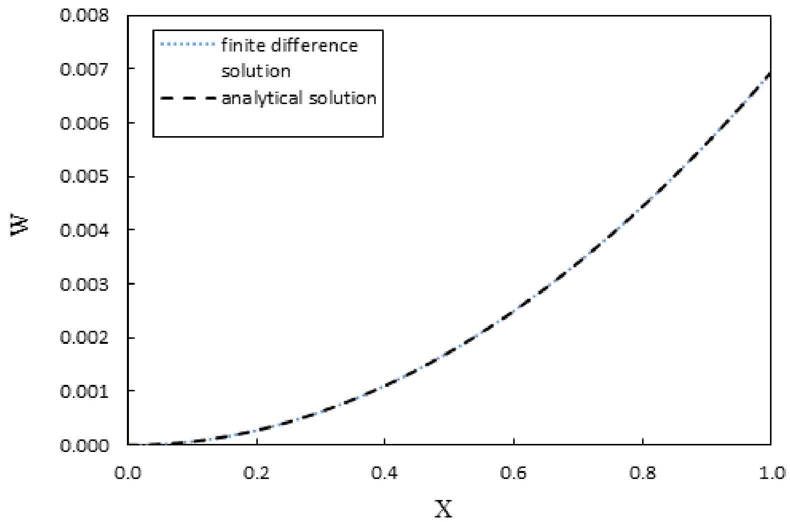

Fig. 8 The finite difference and analytical solutions of the dimensionless transverse deflection of case (1) at η=0.05

thermal moment will be in the form of deflection and thermal strain. No thermal stresses will be generated as long as one end of the slab is maintained free without any constraints or motion restriction. However, equivalent thermal stresses can be obtained to represent the effect of a fictitious counter act mechanical moment applied at the free end of the slab to restraint the deflection. The dimensionless equivalent thermal stress and thermal strain distributions can be obtained by using Eqs. (20)-(21) respectively which indicate identical trends to the dimensionless temperature solution with considering the negative sign in the thermal stress equation.

The dimensionless transverse deflection of the cantilevered slab due to the applied thermal

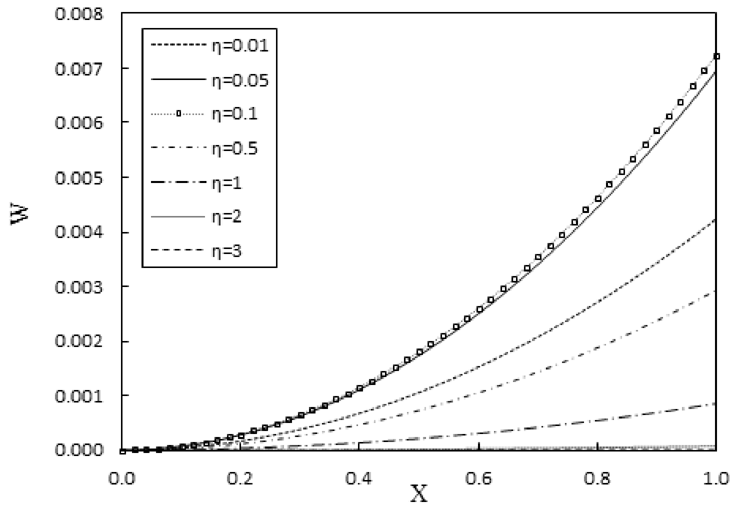

Fig. 9 Transient dimensionless deflection of the slab for case (2) at R=1

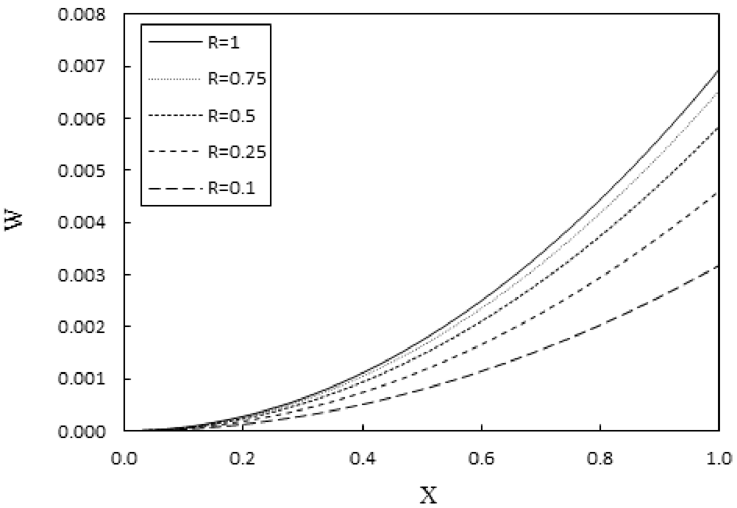

Fig. 10 Dimensionless deflection of the slab for case (2) at different values of R at η=0.05

moment is obtained numerically, through finite difference analysis, by solving the equation of motion (24) and analytically by solving the equilibrium Eq. (25). The numerical and analytical solutions at η=0.05 are shown in Fig. 8 which reveals a perfect match between the two solutions and hence verifies the implemented numerical method.

The transient response of the slab in terms of the dimensionless deflection for case (2) at different time values with R=1 and at different R values with η=0.05 is shown in Figs. 9 and 10 respectively.

Fig. 9 shows that the transverse deflection along the slab increases with time until it reaches its maximum value when η=0.1 then it starts to decrease until it reaches zero at η_{ss}=3 at which the temperature through the thickness of the slab becomes uniform. In another aspect, Fig. 10 confirms

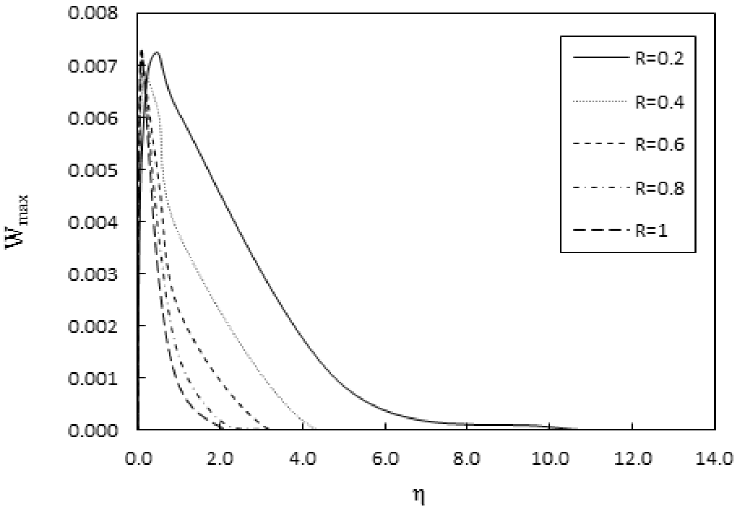

Fig. 11 The maximum dimensionless deflection versus the dimensionless time at different values of *R* for case (2)

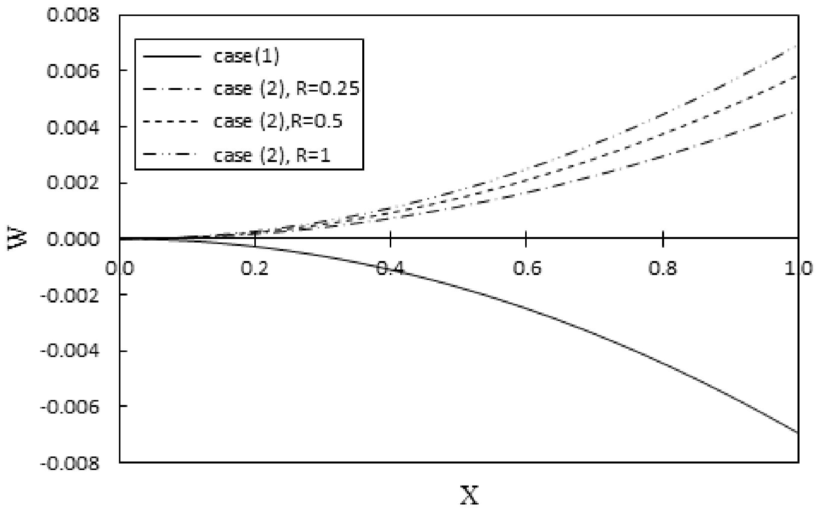

Fig. 12 The alternating dimensionless deflection of the slab at η=0.05

that reducing the value of *R* slows down the heat flow and consequently retards the elastic response.

Fig. 11 presents the variation in the maximum dimensionless deflection at the free end of the slab as time passes on at different values of *R* for case (2).

It is shown in Fig. 11 that the deflection of the free end of the slab increases from zero to maximum and then decreases back to zero at the steady state time. It is also shown that decreasing the value of *R* reduces the response time without affecting the maximum value of the deflection.

The discussion of the results in this study is extended to shed the light on the fluctuating response of the slab due to the reversal in the heat flow direction between cases (1) and (2). Here, the time of applying the heat flow in one direction is considered to be of the same duration as that for the heat flow in the reversed direction. Fig. 12 presents the alternating dimensionless deflection along the slab between case (1) and case (2) for R=1, 0.5 and 0.25 at η=0.05.

If reversing the heat flow direction is applied repeatedly, the slab will be under the effect of a cyclic thermal load and consequently under thermal fatigue. The thermal fatigue can be seen as an alternating change in the magnitude and direction of the deflection, the thermal strain, and/or the thermal stress. The amplitude and the frequency of the fluctuating response determine the severity of the thermal fatigue load. The concerns associated with the thermal fatigue come from the fact that fatigue loads generally produce crack nuclei that are likely to grow and propagate leading to fatigue failure of the solid component. The rate of crack propagation theoretically depends on the amplitude of the fluctuating response and other material and geometric parameters.

In the current problem, the distance traveled by the free end of the slab between cases (1) and (2) while reversing the heat flow direction is considered the range of the fluctuating response. It is shown in Fig. 12 that a slab made of a thermal diode like material with R=0.25 would have a fatigue range, and hence amplitude, smaller than that associated with R=1 which in turns reduces the severity of the thermal fatigue load.

6. Conclusions

The transient thermoelastic response of a clamped-free slab made of a thermal diode-like material and subjected to a thermal load was investigated through analytical and finite difference analyses. The results of the study have shown that reducing the ratio between the low and high thermal conductivity values of the material (R) slows down the rate of heat transfer from one side of the slab to the other. It was also found that the transverse deflection of the slab reaches its maximum when the dimensionless temperature at the insulated side of the slab departs from zero at the critical time and then it goes back to zero at the steady state time. Both the critical time and the steady state time were found to be inversely proportional to R. Finally, the amplitude of deflection due to a thermal fatigue load was found directly proportional to R.

References

Addam, A.M.A (2000), "Temperature and thermal stresses in a two layer slab under the effect of the hyperbolic heat conduction model", M.S. Thesis, Mechanical Engineering Department, Jordan University of Science and technology, Jordan.

Al-Huniti, N.S. and Al-Nimr, M. (2000), "Behavior of thermal stresses in a rapidly-heated thin plate", *J. Therm. Stress.*, **23**, 293-307.

Al-Huniti, N.S., Al-Nimr, M.A. and Naji, M. (2001), "Dynamic response of a rod due to a moving heat source under the hyperbolic heat conduction model", *J. Sound. Vib.*, **242**, 629-640.

Al-Nimr, M.A. and Al-Huniti, N.S. (2000), "Transient thermal stresses in a thin elastic plate due to a rapid dual-phase-lag heating", *J. Therm. Stress.*, **23**, 731-746.

Al-Nimr, M.A. and Abou-Arab, T.W. (1994), "Transient temperature distribution within a flat sheet during the welding process-analytical solution", *Heat Transf. Eng.*, **15**, 27-33.

Boley, B. and Weiner, J. (1985), *Theory of Thermal Stresses*, Krieger, Florida.

Brischetto, S.R., Leetsch, E., Carrera, T. and Wallmersperger, B. (2008), "Thermo-Mechanical bending of functionally graded plates", *J. Therm. Stress*., **31**, 286-308.

Darwish, F.H., AL-Nimr, M.A. and AL-Hunti, N.S. (2012), "Transient response of a clamped slab under pressure and thermal loads", *J. Therm. Stress.*, **35**, 470-484.
Feng, W.J., Pan, E. and Wang, X. (2008), "Stress analysis of a penny-shaped crack in a magneto-electro-thermo-elastic layer under uniform heat flow and shear loads", *J. Therm. Stress.*, **31**, 497-514.
Hata, T. (2001), "Thermal stresses focusing effect following rapid non uniform heating of long cylindrical rods", *J. Therm. Stress.*, **24**(2), 93-104.
Hu, B., Li, H. and Xie, B.S. (2005), "Heat conduction in a one-dimensional Yukawa chain", *Europhys. Lett.*, **69,** 358.
Ieşan, D. (2008), "Thermo-elastic deformation of porous Cosserat beams", *J. Therm. Stress.*, **31**, 823-847.
Kreith, F. and Black, W.A. (1980), *Basic Heat Transfer*, Harper and Row, New York, U.S.A.
Nowacki, W. (1986), *Thermoelasticity*, Second Edition, Pergamon Press, PWN, Warsaw.
Shahani, A.R. and Bashusqeh, S.M. (2013), "Analytical solution of the coupled thermo-elasticity problem in a pressurized sphere", *J. Therm. Stress.*, **36**, 1283-1307.
Suh, C. and Burger, C. (1998), "Thermoelastic modeling of laser-induced stress waves in plates", *J. Therm. Stress.*, **21**, 829-847.
Sumi, N., Hetnarski, R.B. and Noda, N. (1987), "Transient thermal stresses due to a local source of heat moving over the surface of an infinite elastic slab", *J. Therm. Stress.*, **10**, 83-96.
Tall, L. (1964), "Residual stresses in welded plates-a theoretical study", *Weld. J.*, **43**, 10-23.
Terraneo, M., Peyrard, M. and Casati, G. (2002), "Controlling the energy flow in nonlinear lattices: a model for a thermal rectifier", *Phys. Rev. Lett.*, **88**, 094302.
Tzou, D.Y. (1997), *Macro-to Microscale Heat Transfer*, Taylor and Francis, Washington, DC.
Ugural, A.C. (1999), *Stresses in Plates and Shells*, McGraw Hill, New York, U.S.A.
Wang, B., Li, L. and Casati, G. (2004), "Thermal diode: rectification of heat flux", *Phys. Rev. Lett.*, **93**, 184301.
Wang, B., Li, L. and Casati, G. (2006), "Negative differential thermal resistance and thermal transistor", *Phys. Lett.*, **88**, 143501.
Xu, Y., Zhou, D. and Liu, K. (2010), "Three-dimensional thermoelastic analysis of rectangular plates with variable thickness subjected to thermomechanical loads", *J. Therm. Stress.*, **33**, 1136-1155.

CC

Nomenculture

AR	Aspect ratio	z	Transverse coordinate (m)
D	Flexural rigidity (N.m^2)	α_H	High thermal diffusivity (m^2/s)
E	Modulus of elasticity (N/m^2)	α_L	Low thermal diffusivity (m^2/s)
h	Thickness of the slap (m)	β	Fourier coefficient
k_H	High thermal conductivity (W/m.℃)	γ	Coefficient of thermal expansion (1/℃)
k_L	Low thermal conductivity (W/m.℃)	ε_T	Thermal strain
L	Length of the slap (m)	ϵ_T	Dimensionless thermal strain
M_T	Thermal moment (N.m)	η	Dimensionless time
R	Ratio between low and high thermal conductivity	η_{ss}	Dimensionless steady state time
S_T	Dimensionless thermal stress	η_c	Dimensionless critical time
t	Time (s)	θ	Dimensionless temperature
T	Temperature (℃)	θ_{ss}	Dimensionless steady state temperature
T_w	Wall temperature (℃)	λ	Dimensionless parameter

T_∞	Initial temperature (℃)	μ	Dimensionless parameter
w	Transverse deflection (m)	υ	Poisson's ratio
W	Dimensionless transverse deflection	ξ	Dimensionless transverse coordinate
x	Axial coordinate (m)	ρ	Mass density (kg/m^3)
X	Dimensionless axial coordinate	σ_T	Thermal stress (N/m^2)